Published in final edited form as:
Astron Astrophys. 2019 October ; 630: . doi:10.1051/0004-6361/201936372.

Discovery of two new magnesium-bearing species in IRC+10216: MgC_3N and MgC_4H ★

J. Cernicharo[1,★★], **C. Cabezas**[1], **J. R. Pardo**[1], **M. Agúndez**[1], **C. Bermúdez**[1], **L. Velilla-Prieto**[1,2], **F. Tercero**[3], **J. A. López-Pérez**[3], **J. D. Gallego**[3], **J. P. Fonfría**[1], **G. Quintana-Lacaci**[1], **M. Guélin**[4], **Y. Endo**[5]

[1]Grupo de Astrofísica Molecular. Instituto de Física Fundamental (IFF-CSIC). C/Serrano 121, 28006 Madrid, Spain

[2]Department of Space, Earth and Environment, Chalmers University of Technology, Onsala Space Observatory, 439 92 Onsala, Sweden

[3]Centro de Desarrollos Tecnológicos, Observatorio de Yebes (IGN), 19141 Yebes, Guadalajara, Spain

[4]Institut de Radioastronomie Millimétrique, 300 rue de la Piscine, F-38406, Saint Martin d'Hères, France

[5]Department of Applied Chemistry, Science Building II, National Chiao Tung University, 1001 Ta-Hsueh Rd., Hsinchu 30010, Taiwan

Abstract

We report on the detection of two series of harmonically related doublets in IRC +10216. From the observed frequencies, the rotational constant of the first series is $B = 1380.888$ MHz and that of the second series is $B = 1381.512$ MHz. The two series correspond to two species with a $^2\Sigma$ electronic ground state. After considering all possible candidates, and based on quantum chemical calculations, the first series is assigned to MgC_3N and the second to MgC_4H. For the latter species, optical spectroscopy measurements support its identification. Unlike diatomic metal-containing molecules, the line profiles of the two new molecules indicate that they are formed in the outer layers of the envelope, as occurs for MgNC and other polyatomic metal-cyanides. We also confirm the detection of MgCCH that was previously reported from the observation of two doublets. The relative abundance of MgC_3N with respect to MgNC is close to one while that of MgC_4H relative to MgCCH is about ten. The synthesis of these magnesium cyanides and acetylides in IRC +10216 can be explained in terms of a two-step process initiated by the radiative association of Mg^+ with large cyanopolyynes and polyynes followed by the dissociative recombination of the ionic complexes.

★Based on observations carried out with the IRAM 30m telescope and the Yebes 40m telescope. IRAM is supported by INSU/CNRS (France), MPG (Germany) and IGN (Spain). The 40m radiotelescope at Yebes Observatory is operated by the Spanish Geographic Institute (IGN, Ministerio de Fomento).

★★corresponding author. jose.cernicharo@csic.es.

Europe PMC Funders Author Manuscripts

Keywords

molecular data; line: identification; stars: carbon; circumstellar matter; stars: individual (IRC +10216); astrochemistry

1 Introduction

Metal-containing molecules are rarely observed in the interstellar medium, but are widely detected in circumstellar envelopes around evolved stars. Stable closed-shell diatomic molecules containing Al, Na, or K and a halogen atom have been detected in the prototypical carbon star envelope IRC +10216 (Cernicharo & Guélin 1987). These species are mostly formed in the hot inner parts of the envelope, close to the star. Metals like Na, K, Ca, Cr, and Fe are found to survive in the gas phase as neutral and/or ionized atoms in the outer layers of IRC +10216 (Mauron & Huggins 2010), which points to a very rich metal chemistry in the cool outer envelope. Various triatomic metal cyanides (M−NC or/and M −CN) containing Mg, Na, Al, Si, K, Fe, and Ca (most of which are open-shell radicals) have been detected in IRC +10216 (Kawaguchi et al. 1993; Turner et al. 1994; Ziurys et al. 1995, 2002; Guélin et al. 2000, 2004; Pulliam et al. 2010; Zack et al. 2011; Cernicharo et al. 2019). Guélin et al. (1993) studied the spatial distribution of MgNC and concluded that this radical arises from a shell located at 15″ from the star.

The only tetratomic metal-bearing species detected so far in IRC +10216 is HMgNC (Cabezas et al. 2013). A pentatomic species, MgC_3N, was postulated by Petrie et al. (2003) as a potential abundant species in IRC +10216. They suggested that a series of doublets with rotational constant around 1395 MHz, although initially assigned to an electronic excited state of C_6H by Aoki (2000), were in fact produced by MgC_3N. However, Cernicharo et al. (2008) have shown that these doublets certainly belong to the $^2\Sigma$ state of the ν_{11} bending mode of C_6H in its $^2\Pi$ ground electronic state. Nevertheless, MgC_3N, together with MgC_4H, which could be formed in the cold outer layers of IRC +10216, are interesting molecules to be searched for in this object.

Sensitive line surveys can be used as the magic tool to reveal the molecular content of astronomical sources and to search for new molecules. Once we are able to identify the lines coming from the isotopologues and vibrationally excited states of known molecules, then a forest of unidentified lines appear that provide the opportunity to discover new molecules and insights into the chemistry and chemical evolution of the observed object.

In this Letter we report the discovery of two new series of doublets with very close rotational constants (1380.9 MHz and 1381.5 MHz) produced by two new molecular species having a $^2\Sigma$ ground electronic state. On the basis of precise quantum chemical calculations and an exploration of all possible candidates, we assign these lines to MgC_3N and MgC_4H.

2 Observations

The observations at 3 mm presented in this paper were carried out with the IRAM 30m radio telescope and have been described in detail by Cernicharo et al. (2019). Briefly, the data in

Europe PMC Funders Author Manuscripts

the 3 mm window correspond to observations acquired during the last 35 years and cover the 70-116 GHz domain with very high sensitivity (1-3 mK). Examples of these data can be found in Cernicharo et al. (2004, 2007, 2008, 2019) and Agúndez et al. (2008, 2014). The observing mode, where we wobbled the secondary mirror by ±90” at a rate of 0.5 Hz, ensured flat baselines. This observing method provides reference data free from emission from all molecules but CO (see Cernicharo et al. 2015). The emission of all other molecular species is restricted to a region ≤ 15-20″ from the star (see e.g. Guélin et al. 1993; Agúndez et al. 2015, 2017; Velilla Prieto et al. 2015; Quintana-Lacaci et al. 2016).

The observations in the Q band (32-50 GHz) were performed in May and June 2019 with the 40m radiotelescope of the Centro Astronómico de Yebes (IGN, Spain). New receivers built for the European Research Council synergy project Nanocosmos were installed at the telescope and used for these observations during its commissioning phase. The experimental set-up will be described in detail by Tercero et al. (2019). Briefly, the Q-band receiver consists of two HEMT cold amplifiers covering the 32-50 GHz band with horizontal and perpendicular polarizations. Receiver temperatures vary from 22 K at 32 GHz up to 42 K at 50 GHz. The spectrometers are 16 × 2.5 GHz FFTs with a spectral resolution of 38.1 kHz providing the whole coverage of the Q-band in both polarizations. The total observing time on-source for the observations presented here corresponds to ~ 24 h. The observing mode was position switching with an off position at 300″ in azimuth.

Pointing corrections were obtained by observing strong nearby quasars and the SiO masers of R Leo. Pointing errors were always within 2-3″. The intensity scale, antenna temperature (T_A^*), was corrected for atmospheric absorption using the ATM package (Cernicharo 1985; Pardo et al. 2001). The beam size of the IRAM 30m telescope in the 3mm domain is 21-30″, while for the 40m telescope the beam size in the Q band is in the range 36-56″. The main beam efficiency of the 40m telescope varies between 60 % at 32 GHz and 50 % at 50 GHz. Calibration uncertainties of 10% were adopted for data covering such a long observing period in the 3 mm domain. A similar uncertainty was assumed for the data in the Q band. Additional uncertainties could arise from the line intensity fluctuation with time induced by the variation of the stellar infrared flux (Cernicharo et al. 2014; Pardo et al. 2018). All data were analysed using the GILDAS package[1].

3 Results

In the IRAM 30m data we found a series of doublets (S 1) whose components are separated by ~4.3 MHz. The doublets are in harmonic relation with integer quantum numbers from N_{up}=26 to N_{up}=40. Some of these doublets show some overlap with other features, as shown in Figs. 1 and 2. As a first step we verified that no other harmonic relation can apply and the lines cannot be due to any known species. Once we were sure that the doublets belong to a new molecular species, we searched for the corresponding doublets in the Q band, which correspond to quantum numbers from N_{up}=12 to N_{up}=18. All them were detected and are shown in Fig. 1. Interestingly, none of these doublets are present in the previous survey of IRC +10216 in the Q band performed with the Nobeyama radiotelescope (Kawaguchi et al.

[1] http://www.iram.fr/IRAMFR/GILDAS

1995). This is due to the higher sensitivity of our data, less than 1 mK (see Fig. 1) versus 5 mK in the Nobeyama data. Finally, a total of 22 doublets (see Figs. 1 and 2) were found between the Q and the 3 mm bands. Their frequencies are given in Table A.1 of Appendix A. From a fit to the observed frequencies, we obtain the following rotational, distortion, and spin-rotation constants:

B = 1380.888 ± 0.001 MHz

D = 0.0760 ± 0.0005 kHz

γ = 4.35 ± 0.04 MHz

After a careful examination of the data we realized that some unidentified features located on the right side of the $S1$ doublets are in fact harmonically related doublets with integer quantum numbers ($S2$). They are indicated by magenta arrows in Figs. 1 and 2. The $S2$ doublets have the same quantum numbers as $S1$ and correspond to a $^2\Sigma$ molecule. The frequencies of $S2$, given in Table A.2 of Appendix A, are fitted with the following constants:

B = 1381.512 ± 0.004 MHz

D = 0.074 ± 0.002 kHz

γ = 4.7 ± 0.1 MHz

A detailed analysis of possible carriers for $S1$ and $S2$ is given in Appendix B. After discarding all plausible molecular species, we conclude that our best candidates are metal-bearing species attached to a C_3N or C_4H group. Species containing Na or Al attached to C_3N or C_4H groups have singlet ground electronic states and therefore cannot be the carriers of $S1$ and $S2$. In fact, AlC_3N and NaC_3N have been observed in the laboratory (Cabezas et al. 2014, 2019) and their rotational constants are too low with respect to those quoted above for $S1$ and $S2$. In contrast, molecular species containing Mg or Ca present $^2\Sigma$ electronic states and they are postulated as the candidates responsible for the $S1$ and $S2$ rotational transitions. In a previous paper, Cabezas et al. (2019) reported ab initio calculations for both MgC_3N and CaC_3N species. The calculated rotational constant for MgC_3N indicates that this molecule could be one of the carriers of $S1$ or $S2$. On the other hand, the rotational constant of CaC_3N is much smaller than those of $S1$ and $S2$, discarding Ca as a candidate. Hence, we performed high-level quantum chemical calculations for both MgC_4H and MgC_3N (see Appendix C). For MgC_3N we obtain B = 1376.5 MHz, D = 0.065 kHz, and γ = 4.1 MHz. For MgC_4H we obtained a slightly higher value of B, 1377.4 MHz, D = 0.061 kHz, and γ = 4.4 MHz. All these results are given in Appendix C.

High-resolution optical spectroscopy of the $A^2\Pi - X^2\Sigma$ electronic transition of MgC_4H were performed by Ding et al. (2008) and Chasovskikh et al. (2008). They obtain a rotational constant of B = 1384.7 ± 6 MHz. Subsequent observations of the same electronic transition of MgC_4H by Forthomme et al. (2010) provide a much more accurate value for the rotational constant, B = 1380.9 ± 0.2 MHz. The spectral resolution of these observations is 0.002 cm^{-1} (~60 MHz) and near 250 transitions have been observed with upper quantum

numbers up to $N = 42$. Hence, the derived rotational constant and its uncertainty are highly confident. Using the relation $D = B^3/\omega^2$, these authors estimated the distortion constant to be 0.077 kHz. Hence, either of the two series $S1$ or $S2$ may be assigned to MgC_4H. The calculated dipole moment of MgC_3N is 6.3 D and that of MgC_4H 2.1 D (see Appendix C). Consequently, both species will harbour a different line intensity distribution with quantum number N. We consider that MgC_4H is responsible for the $S2$ series as its dipole moment of 2.1 D produces rotational transitions in IRC +10216 peaking in the 3 mm domain with weak emission below 50 GHz. Consequently, the $S1$ series is assigned to MgC_3N because with its high dipole moment its rotational transitions are strong in the Q band and will start to decline in intensity for high values of N in the 3mm band (similar to the behaviour of HC_5N). Moreover, all quantum chemical calculations indicate that the rotational constant of MgC_4H is slightly larger than that of MgC_3N, as observed for $S2$ and $S1$. Consequently, we conclude that we have detected, and fully characterized spectroscopically in space, the magnesium-bearing species MgC_3N ($S1$) and MgC_4H ($S2$). The definitive confirmation will require laboratory rotational spectroscopy. We also present new observations (see Appendix E) that confirm the tentative detection of MgCCH in IRC +10216 reported by Agúndez et al. (2014).

4 Discussion

The observed line intensities of MgC_3N can be fit to two components, a cold one with a rotational temperature of 15 ± 2 K and a column density of $(5.7 \pm 1.0) \times 10^{12}$ cm^{-2}, and a warm one with $T_{rot} = 34 \pm 6$ K and $N = (3.6 \pm 0.6) \times 10^{12}$ cm^{-2}. For MgC_4H we derive a relatively high rotational temperature (36±6 K), which is consistent with the line intensity distribution quoted above, and a column density of $(2.2 \pm 0.5) \times 10^{13}$ cm^{-2}. The determination of column densities can be quite uncertain if infrared pumping (IR) plays a role in the excitation of the rotational levels (see Appendix D). These effects could be particularly important for molecules having low-frequency bending modes such as HC_3N, HC_5N, C_4H, MgC_3N, and MgC_4H (see Appendix D). Nevertheless, our two magnesium-bearing species have similar low-frequency bending modes (see Tables C.3 and C.4) and we could expect to have similar effects in the infrared pumping of their rotational levels. Therefore, the ratio of column densities MgC_4H/MgC_3N ~2.5 should not be greatly affected by IR pumping effects. On the other hand, the abundance ratio $MgC_4H/MgCCH$ ~10 may be overestimated if IR pumping is important for MgC_4H (see Appendices D and E). It is true that it seems counterintuitive to have a higher abundance for MgC_4H than for MgCCH, but in the chemical model discussed below everything depends on the branching ratios of the different fragmentation channels in the dissociative recombination of the $MgC_{2n}H_2^+$ complexes, which are difficult to anticipate (see below). Usually, within a given chemical family, larger molecules tend to be less abundant in IRC+10216. However, the anions C_nH^-, for which their synthesis also relies on the radiative association of C_nH radicals and electrons, show an increase in abundance with the number of carbon atoms.

In order to investigate the formation of the various magnesium cyanides and acetylides detected in IRC +10216 (MgNC, MgCN, HMgNC, MgC_3N, MgCCH, and MgC_4H) we carried out chemical model calculations based on the model of the outer envelope by

Agúndez et al. (2017). As in previous models dealing with the formation of metal-bearing molecules in the outer shells of IRC +10216 (Millar 2008; Cabezas et al. 2013; Cernicharo et al. 2019), the synthesis relies on a two-step mechanism starting with the radiative association of Mg^+ with large cyanopolyynes and polyynes and the subsequent dissociative recombination of the corresponding $Mg^+/NC_{2n+1}H$ and $Mg^+/C_{2n}H_2$ complexes with electrons (Petrie 1996).

The rate coefficients for the radiative associations of Mg^+ with polyynes and cyanopolyynes were taken from the calculations by Dunbar & Petrie (2002). We consider that open-shell metal-containing species (MgNC, MgCN, MgC_3N, MgCCH, and MgC_4H) react with electrons and H atoms, while closed-shell molecules (HMgNC) do not. The branching ratios of the different fragmentation channels in the dissociative recombination of the $Mg^+/NC_{2n+1}H$ and $Mg^+/C_{2n}H_2$ ions are not known. We have therefore adjusted them to obtain column density ratios in agreement with those derived from observations. We find that in order to reproduce the relative column densities of the magnesium cyanides, the branching ratios of the channels yielding HMgNC, MgCN, and MgC_3N should respectively be 0.01, 0.05, and 0.7 of that yielding MgNC. In the case of the magnesium acetylides, the branching ratio of the channel producing MgCCH should be 0.1 of that yielding MgC_4H. It is curious that while MgNC is slightly more abundant than MgC_3N, in the case of magnesium acetylides the larger molecule MgC_4H is significantly more abundant than MgCCH. If the conclusion of $MgC_4H/MgCCH > 1$ is not in error due to IR pumping effects, this should be a consequence of the different behaviour in the fragmentation of $Mg^+/C_{2n}H_2$ complexes with respect to $Mg^+/NC_{2n+1}H$.

The absolute column densities of the Mg-bearing molecules are approximately reproduced (calculated column densities for MgC_3N and MgC_4H are 5.4×10^{12} and 3.6×10^{13} cm^{-2}, respectively) adopting an initial abundance of Mg relative to H of 1.5×10^{-6}, which is about 4 % of the cosmic abundance of Mg. This value is higher than that used by Cabezas et al. (2013), mainly because in this model we include more metals (Mg, Na, Al, and Ca) and the new and abundant detected molecule MgC_3N must be accounted for. Unfortunately, Mauron & Huggins (2010) did not observe atomic Mg in the outer layers of IRC +10216, and therefore we do not have constraints on the abundance of atomic Mg. The results from the chemical model are shown in Fig. 3. In general, the two-step mechanism of Petrie (1996) can account for the formation of Mg cyanides and acetylides in IRC +10216. The main uncertainty is related to the branching ratios of the different fragmentation channels in the dissociative recombination of the cationic metal complexes, something that would be worth investigating in detail in the future.

Supplementary Material

Refer to Web version on PubMed Central for supplementary material.

Acknowledgements

The Spanish authors thank the Ministerio de Ciencia Innovación y Universidades for funding support from the CONSOLIDER-Ingenio program ‘ASTROMOL’ CSD 2009-00038, AYA2012-32032, AYA2016-75066-C2-1-P. We also thank ERC for funding through grant ERC-2013-Syg-610256-NANOCOSMOS. MA thanks the Ministerio de

Ciencia Innovación y Universidades for the Ramón y Cajal grant RyC-2014-16277. CB thanks the Ministerio de Ciencia Innovación y Universidades for the Juan de la Cierva grant FJCI-2016-27983. LVP acknowledges support from the Swedish Research Council and from ERC consolidator grant 614264.

References

Adler TB, Knizia G, Werner H-J. J Chem Phys. 2007; 127:221106. [PubMed: 18081383]
Agúndez M, Cernicharo J. ApJ. 2006; 650:374.
Agúndez M, Fonfría JP, Cernicharo J, et al. A&A. 2008; 479:493.
Agúndez M, Cernicharo J, Guélin M. A&A. 2014; 570:45.
Agúndez M, Cernicharo J, Quintana-Lacaci G, et al. ApJ. 2015; 814:143.
Agúndez M, Cernicharo J, Quintana-Lacaci G, et al. A&A. 2017; 601:A4.
Aoki K. Chem Phys Lett. 2000; 323:55.
Bacalla X, Salumbides EJ, Linnartz HH, et al. J Phys Chem A. 2016; 120:6402. [PubMed: 27459295]
Bjorvatten T. J Mol Structure. 1974; 20:75.
Brewster MA, Apponi AJ, Xin J, Ziurys LM. Chem Phys Lett. 1999; 310:411.
Cabezas C, Cernicharo J, Alonso JL, et al. ApJ. 2013; 775:133.
Cabezas C, Barrientos C, Largo A, et al. J Chem Phys. 2014; 141:104305. [PubMed: 25217914]
Cabezas C, Barrientos C, Largo A, et al. J Chem Phys. 2019; doi: 10.1063/1.5110670
Castor JI. MNRAS. 1970; 149:111.
Cernicharo, J. Internal IRAM report. Granada: IRAM; 1985.
Cernicharo J, Guélin M, Kahane C, et al. A&A. 1991; 246:213.
Cernicharo J, Guélin M. A&A. 1987; 183:L10.
Cernicharo J, Guélin M, Kahane C. A&AS. 2000; 142:181.
Cernicharo J, Guélin M, Pardo JR. ApJ. 2004; 615:L145.
Cernicharo J, Guélin M, Agúndez M, et al. A&A. 2007; 467:L37.
Cernicharo J, Guélin M, Agúndez M, et al. ApJ. 2008; 688:L83.
Cernicharo, J. In: Stehl, C; Joblin, C; d'Hendecourt, L, editors. ECLA 2011; Proc of the European Conference on Laboratory Astrophysics, EAS Publications Series, 2012; Cambridge: Cambridge Univ Press; 2012. https://nanocosmos.iff.csic.es/?page_id=1619
Cernicharo J, Teyssier D, Quintana-Lacaci G, et al. ApJ. 2014; 796:L21.
Cernicharo J, Marcelino N, Agúndez M, Guélin M. A&A. 2015; 575:A91.
Cernicharo J, Guélin M, Agúndez M, et al. A&A. 618:A4.
Cernicharo J, Velilla-Prieto L, Agúndez M, et al. A&A. 2019; 627:L4.
Chasovskikh E, Jochnowitz EB, Maier JP. J Phys Chem A. 2008; 112:8686. [PubMed: 18729429]
Ding H, Apetrei C, Chacaga L, Maier JP. ApJ. 2008; 677:348.
Dunbar RC, Petrie S. ApJ. 2002; 564:792.
Frisch MJ, Trucks GW, Schlegel HB, et al. Gaussian 16 rev A. 2016:03.
Forthomme D, Linton C, Tokaryk DW, et al. Chem Phys Lett. 2010; 488:116.
Gou X, Zhang J, Li J, et al. Chem Phys. 2009; 360:27.
Guélin M, Lucas R, Cernicharo J. A&A. 1993; 280:L19.
Guélin M, Muller S, Cernicharo J, et al. A&A. 2000; 363:L9.
Guélin M, Muller S, Cernicharo J, et al. A&A. 2004; 426:L49.
Hill JG, Mazumder S, Peterson KA. J Chem Phys. 2010a; 132:054108. [PubMed: 20136306]
Hill JG, Peterson KA. Phys Chem Chem Phys. 2010b; 12:10460. [PubMed: 20603665]
Jerosimić S, Wester R, Gianturco FA. PCCP. 2019; 21:11405. [PubMed: 31111134]
Kawaguchi K, Kasai Y, Ishikawa S, Kaifu N. Pub Astron Soc Japan. 1995; 47:853.
Kawaguchi K, Kagi E, Hirano T, et al. ApJ. 1993; 406:L39.
Knizia G, Adler TB, Werner H-J. J Chem Phys. 2009; 130:054104. [PubMed: 19206955]
McCarthy MC, Apponi AJ, Gottlieb CA, et al. J Chem Phys. 2001; 115:870.

Millar TJ. Ap&SS. 2008; 313:223.
Mauron N, Huggins PJ. A&A. 2010; 513:A31.
Pardo JR, Cernicharo J, Serabyn E. IEEE Trans Antennas and Propagation. 2001; 49:12.
Pardo JR, Cernicharo J, Velilla-Prieto L, et al. A&A. 615:L4.
Petrie S. MNRAS. 1996; 282:807.
Petrie S. MNRAS. 1999; 302:482.
Petrie S, Kagi E, Kawaguchi K. MNRAS. 2003; 343:209.
Pulliam RL, Savage C, Agúndez M, et al. ApJ. 2010; 725:L181.
Quintana-Lacaci G, Agúndez M, Cernicharo J, et al. A&A. 2016; 592:A51.
Sobolev, VV. Cambridge: Harvard University Press; 1960.
Sumiyoshi Y, Katoh K, Endo Y. Chem Phys Lett. 2005; 414:82.
Tercero F, et al. 2019
Turner B, Steimle TC, Meerts L. ApJ. 1994; 426:L97.
Umeki H, Nakajima M, Endo Y. J Chem Phys. 2014; 141:184303. [PubMed: 25399143]
Velilla Prieto L, Cernicharo J, Quintana-Lacaci G, et al. ApJ. 2015; 805:L13.
Werner H-J, Knowles PJ, Knizia G, et al. MOLPRO version 2018. 2018; 1
Zack LN, Halfen DT, Ziurys LM. ApJ. 2011; 733:L36.
Ziurys LM, Apponi AJ, Guélin M, Cernicharo J. ApJ. 1995; 445:L47.
Ziurys LM, Savage C, Highberger JL, et al. ApJ. 2002; 564:L45.

Europe PMC Funders Author Manuscripts

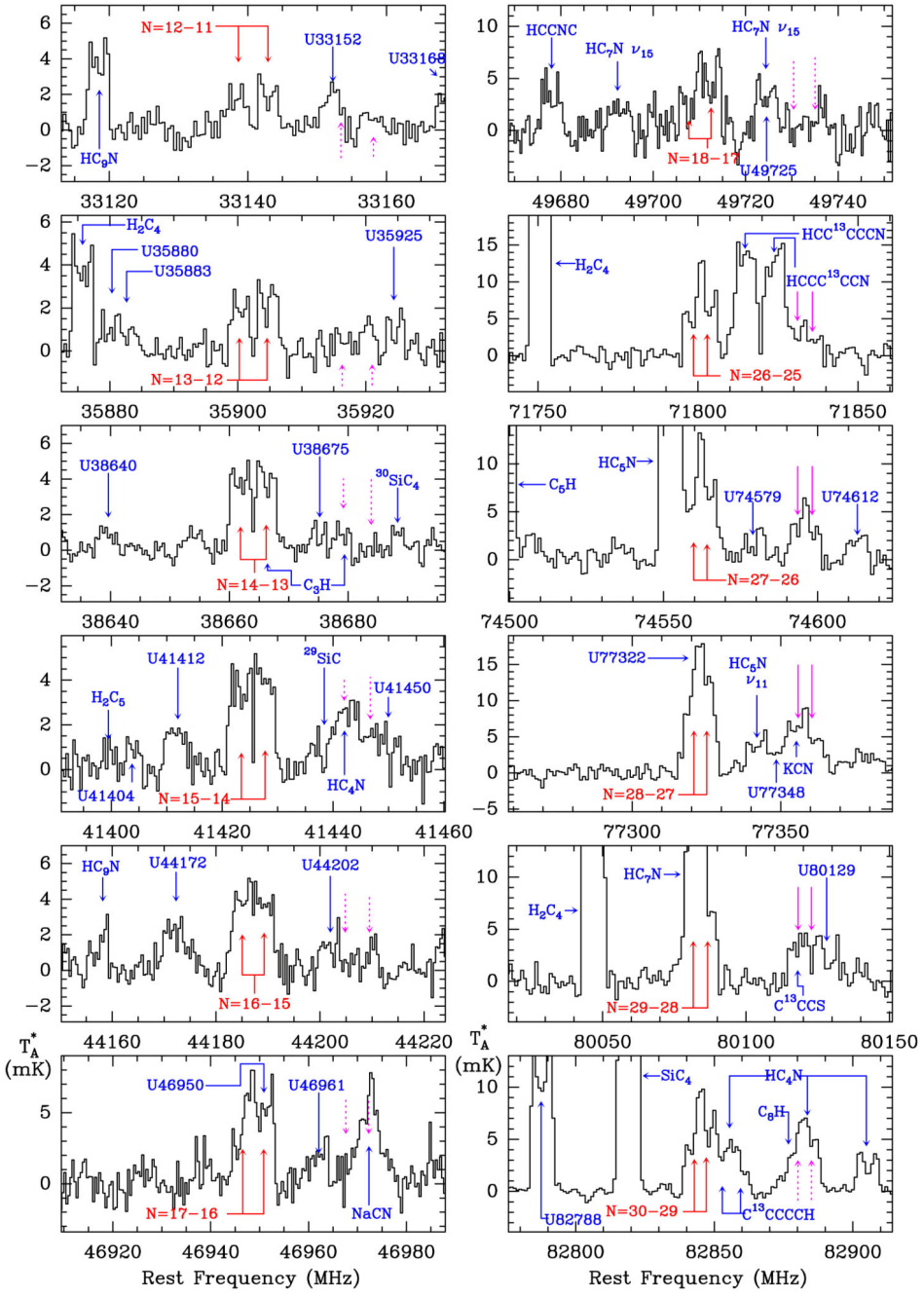

!0.71

Fig. 1.

Observed doublets towards IRC+10216 (black histogram). The vertical scale is the antenna temperature in mK and the horizontal scale is the rest frequency in MHz. Shown are the lines of the series of doublets $S1$ (labelled in red) and those of series $S2$, with the same quantum numbers as $S1$ (in magenta); unidentified (U) lines and lines arising from other species are also shown (in blue). When lines of the $S2$ series are blended with other features, or are too weak to be detected (those below 50 GHz), their positions are indicated by dashed arrows.

Europe PMC Funders Author Manuscripts

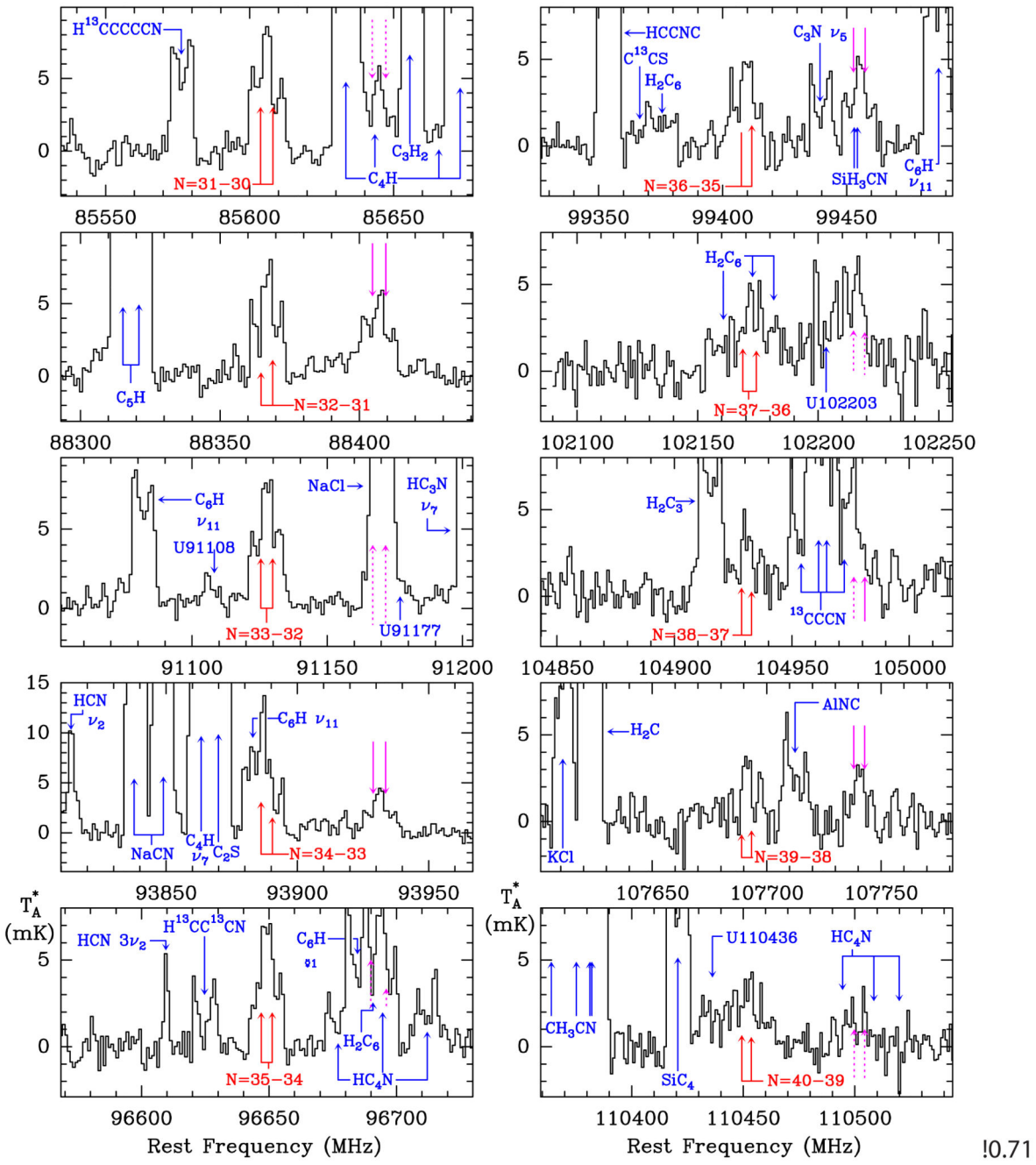

Fig. 2.

Same as in Figure 1, but for the doublets in the 3 mm domain observed with the IRAM 30m radio telescope.

Europe PMC Funders Author Manuscripts

Europe PMC Funders Author Manuscripts

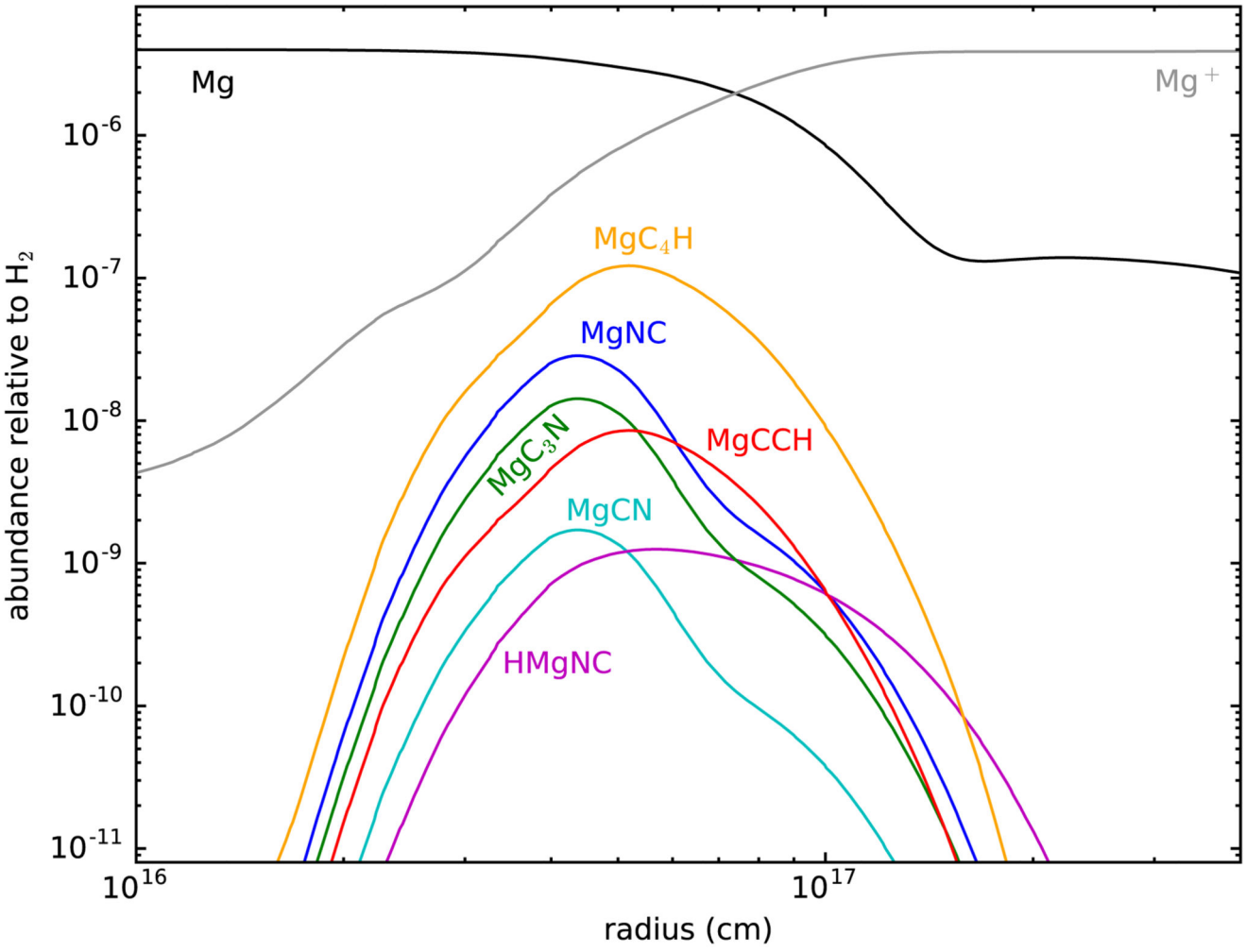

Fig. 3.

Abundances calculated with the chemical model for the different Mg-bearing molecules detected in IRC +10216.